

# A NEW 2D ISOTROPIC LEFT-HANDED METAMATERIAL DESIGN: THEORY AND EXPERIMENT

R. Marqués,<sup>1</sup> J. Martel,<sup>2</sup> F. Mesa,<sup>3</sup> and F. Medina<sup>1</sup>

<sup>1</sup> Dept. de Electrónica y Electromagnetismo  
Universidad de Sevilla

41012 Sevilla, Spain  
<sup>2</sup> Dept. de Física Aplicada II  
Universidad de Sevilla

41012 Sevilla, Spain  
<sup>3</sup> Dept. de Física Aplicada I  
Universidad de Sevilla

Received 31 May 2002

**ABSTRACT:** A novel design for 2D isotropic left-handed metamaterials is presented. One of the main advantages of our proposal is that all the metallizations are placed at parallel stratified planes. Thus, this design can be realized by means of the well known, commonly used planar technology. An analytical model is provided for the analysis of this new metamaterial. Numerical results obtained by using this model are validated by experimental simulations. © 2002 Wiley Periodicals, Inc. *Microwave Opt Technol Lett* 35: 405–408, 2002; Published online in Wiley InterScience (www.interscience.wiley.com). DOI 10.1002/mop.10620

**Key words:** left-handed metamaterials; negative magnetic permeability media

## 1. INTRODUCTION

Electrodynamics of media having dielectric permittivity  $\epsilon$  and magnetic permeability  $\mu$  (both negatives) was theoretically analyzed by Veselago in 1968 [1]. Since the  $\mathbf{E}$ ,  $\mathbf{H}$  fields and the wavevector  $\mathbf{k}$  form a left-handed system in these media, Veselago called them left-handed media (LHM). Backward-wave propagation, negative refractive index, and reverse Doppler effect are, among others, relevant properties of these media. Recently, Smith et al. have experimentally realized an LHM [2]. This medium was built up as the superposition of an artificial plasma medium operating below the plasma frequency and a negative magnetic permeability medium (NMPM). The artificial plasma medium used in the experimental setup was an array of metallic posts sandwiched between two metallic plates. The NMPM was made by inserting a regular array of split ring resonators (SRRs) [3] between the posts. The resulting composite medium shows left-handed wave propagation for certain direction of propagation and polarization of the incident wave. Thus, this medium could be viewed instead as a one-dimensional (1D) LHM, since it presents the wave-propagation features of LHM. However, other LHM effects such as negative refractive index [4] or lens behavior [5] require, at least a 2D realization. Recently, a 2D LHM design has been reported in [6]. This design, which is a modification of Smith's previous design [2], involves a square array of SRRs and metallic strips sandwiched between two parallel upper and bottom metallic plates. The whole structure was reported to be left-handed for wave propagation parallel to the metallic plates and electric field polarization parallel to the metallic strips. However, the above design has some practical disadvantages derived mainly from its non-planar nature (all metallic inclusions must be printed in planes perpendicular to the plane of the structure). Moreover, the edge-coupled SRR (EC-SRR) used to form the NMPM was recently reported to be a bi-anisotropic particle [7]. In consequence, its use in the design of LHM gives rise to the anisotropy and/or bi-(iso/aniso)tropy of the medium [7].

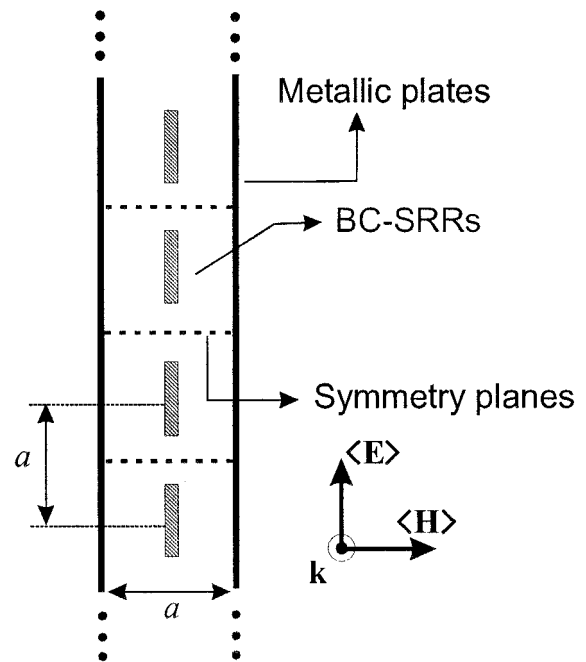


**Figure 1** Front view of the proposed 2D left-handed metamaterial design. The structure is periodical in the direction perpendicular to the plane of the figure, with lattice parameter  $a$ . The field polarization of the macroscopic mean fields in the unit cell is shown as well as the wavevector for the left-handed wave

This paper presents a novel design for 2D isotropic LHM that substantially simplifies previous realizations. In our design, all metallizations are parallel to the plane of the structure thus simplifying its fabrication. Moreover, the bi-anisotropic EC-SRRs are substituted by broadside-coupled SRRs (BC-SRRs), which do not show cross-polarization effects [7]. It will be also shown that the proposed structure presents a left-handed behavior for wave propagation and electric field polarization both parallel to the plane of BC-SRRs.

## 2. ANALYSIS

The proposed structure is a parallel-plate waveguide of spacing  $a$  filled by a 2D cubic array of BC-SRRs, with lattice parameter also equal to  $a$ . The whole structure is sketched in Figure 1 and an individual BC-SRR is shown in detail in Figure 2. Before analyzing the whole structure, the parallel-plate waveguide without the BC-SRRs will be considered. For wave propagation and field polarization both parallel to the plates, the parallel-plate waveguide supports a  $TE_{01}$  mode whose phase constant is given by

$$k = \omega \sqrt{\mu_0 \epsilon_{eff}(\omega)}, \quad (1)$$

where  $\epsilon_{eff}$  is an effective dielectric constant that can be expressed as

$$\epsilon_{eff}(\omega) = \epsilon_0 \left( 1 - \frac{\omega_c^2}{\omega^2} \right), \quad (2)$$

with  $\omega_c$  being the cutoff frequency given by  $\omega_c \sqrt{\epsilon_0 \mu_0} = \pi/a$ . It can be observed that the effective dielectric constant of the parallel-plate waveguide is negative for frequencies below  $\omega_c$  and shows the same frequency dependence as a plasma with plasma

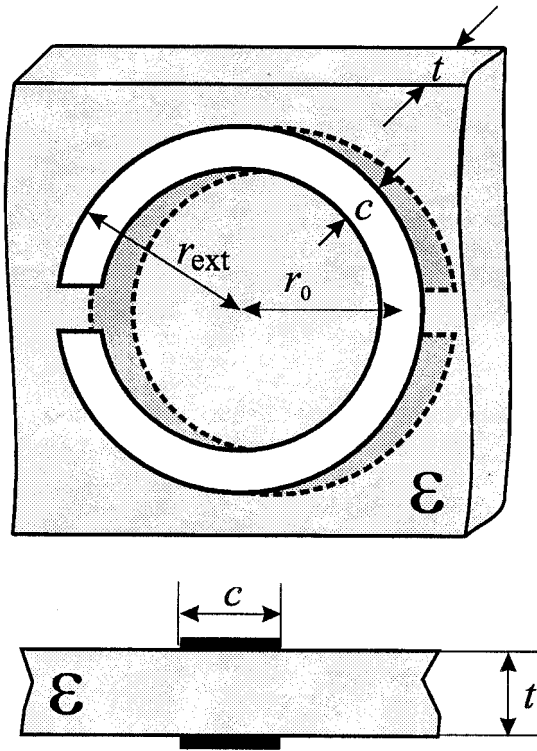


**Figure 2** Detailed picture of one of the BC-SRRs of Fig. 1. The metallic rings are printed on the opposite sides of a dielectric slab of thickness  $t$ . The structural parameters used for the numerical calculations and the experiments are  $r_{\text{ext}} = 2.3$  mm,  $c = 0.5$  mm,  $t = 0.49$  mm and  $\epsilon = 2.43 \epsilon_0$

frequency  $\omega_c$ . This analogy is strengthened by the fact that a surface polarization density on the plates can be defined as the time integral of the surface current density:  $j\omega\mathbf{P}_s = \mathbf{J}_s$ . From this definition and after some calculations, it is finally obtained that the mean volume polarization density  $\langle \mathbf{P} \rangle$  and the mean electric field  $\langle \mathbf{E} \rangle$  in the waveguide cross-section are related (for the aforementioned  $TE_{01}$  mode) by an effective dielectric susceptibility  $\chi_e = -\epsilon_0\omega_c^2/\omega^2$ . This value of  $\chi_e$  exactly coincides with the expected value for a plasma. Thus it can be concluded that a parallel-plate metallic waveguide perfectly simulates a 2D isotropic plasma for wave propagation and electric field polarization both parallel to the plates.

The whole structure shown in Figure 1 is now considered (i.e., the parallel-plate waveguide filled by the BC-SRRs) and laterally extended to form the infinite array displayed in Figure 3. Clearly, the electromagnetic behavior of the structures shown in Figures 1 and 3 must be identical for the aforementioned wave propagation and polarization. If the plates are removed, the resulting medium is a cubic array of BC-SRRs, which is known to behave as a NMPM within certain frequency range [3, 2, 7]. Since the BC-SRR does not show cross-polarization effects [7], this NMPM will be isotropic in the plane of the BC-SRRs (for wave propagation and electric field polarization both parallel to the plane of the structure). Thus, by an appropriate choice of the structural parameters, it should be possible that the whole array of Figure 3 (and therefore the device of Figure 1) behaves as the superposition of a NMPM and an artificial plasma with negative dielectric constant; namely, as a composite LHM [2]. Once this possibility has been shown, the physical constraints on the structural parameters must be determined. First of all, the cutoff frequency  $\omega_c$  must be higher than the resonance frequency  $\omega_0$  of the BC-SRRs [7]. This fact imposes an

upper limit for the lattice parameter  $a$ . Obviously the total dimensions of the BC-SRRs must be smaller than  $a$ . Finally, the electrical size of the BC-SRRs near  $\omega_0$  (where the NMPM behavior occurs) must be small in order to ensure the suitability of the continuum medium approach.

The numerical analysis of the proposed structure follows the main guidelines reported in [7] (a detailed analysis of both the BC-SRR and the EC-SRR was presented in that paper). In particular, the resonance frequency is given by [7]:

$$\omega_0^2 = \frac{2}{\pi r_0 C_{\text{p.u.l.}} L} \quad (3)$$

Closed expressions for the polarizabilities of the BC-SRRs can be also found in [7] (these expressions are the same for both the BC-SRR and the EC-SRR, except for the cross-polarizabilities, which vanishes for the BC-SRR). All these expressions are given as functions of the total inductance of the SRR,  $L$ , and p.u.l. capacitance between the rings  $C_{\text{p.u.l.}}$ . A numerical code has been developed in order to compute these quantities as well as the BC-SRR polarizabilities. The p.u.l. capacitance between the rings is calculated using the design formulas given in [8] (Table 2.6) for the single microstrip transmission line. The total inductance of the BC-SRR is approximated by the inductance of a single ring with the same width and radius. This latter parameter is computed making use of the variational formula  $L = 2U_M/I^2$ , where  $U_M$  is the total self-energy of the ring and  $I$  its total current (the current was taken as uniform in the above calculations). This approximation provides accurate enough results in most cases because of the variational nature of the expression for  $L$ . Once the individual BC-SRR polarizabilities have been found, a suitable homogenization procedure has to be used for obtaining the susceptances of the composite NMPM and/or LHM. However, since the numerical results for both the NMPM and the composite LHM only shows a very slight dependence on the homogenization procedure (see Fig. 2 of [7]), we have finally opted for computing the susceptibilities by simply dividing the polarizabilities of a single BC-SRR

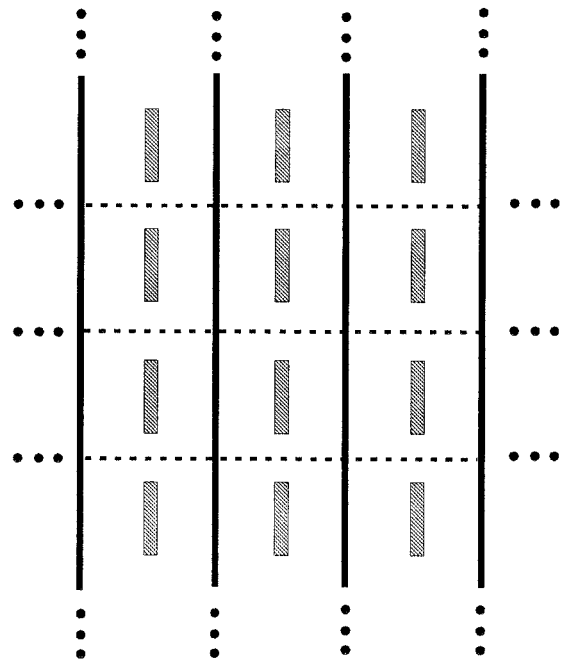


**Figure 3** A bulk LHM made by repetition of the basic design of Fig. 1

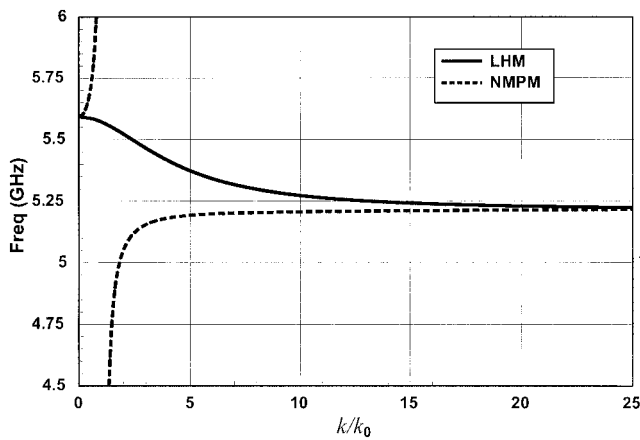


**Figure 4** Numerical results for the normalized phase constant (to  $k_0$ , the free-space wavenumber) of the left-handed wave in the LHM of Figs. 1 and 3. The normalized phase constant for waves propagating in the NMPM medium obtained after removing the metallic plates in Fig. 3 is also shown

by the volume of the unit cell  $a^3$ . This simple procedure has shown to give a good approximation to the medium behavior, at least in a first order approach [7].

### 3. NUMERICAL AND EXPERIMENTAL RESULTS

Following the above numerical procedure, Figure 4 shows the computed results for the normalized phase constant of the 2D LHM of Figure 1 and 3 (a lattice parameter  $a = 6$  mm was chosen and the BC-SRR geometrical dimensions are shown in Figure 2). A left-handed passband, corresponding to a region with effective  $\epsilon$  and  $\mu$  both negatives is predicted just above the resonant frequency for a single BC-SRR. This pass-band extends for several hundreds of MHz. Backward wave propagation can be clearly observed within this passband. Figure 4 also shows the numerical results for the phase constant of the infinite NMPM obtained after removing the plates in Figure 2. The stop-band for the NMPM exactly matches the passband for the LHM. This fact is a consequence of the absence of cross-polarization effects in the BC-SRR [7].

In order to validate our theory, some experiments were carried out. The resonant frequency of an individual BC-SRR of the structure under study was measured by placing it inside a hollow rectangular waveguide. The first resonance was measured experimentally at 5.45 GHz, thus showing a reasonable agreement with the approximated theoretical predictions (see Fig. 4).

An experimental setup was also designed in order to verify the existence of the left-handed passband predicted in Figure 4. In order to simulate the behavior of the 2D LHM of Figures 1 and 3, this setup takes advantage of the presence of planes of symmetry between the BC-SRRs and perpendicular to the plates (these planes are marked with dashed lines in Figures 1 and 3). Taking wave polarization and propagation into account, perfect metallic plates can be located at these planes without affecting the field configuration. Accordingly, the electromagnetic behavior of the 2D LHM can be perfectly simulated by means of a BC-SRR loaded square metallic waveguide whose walls are the actual metallic plates and two adjacent planes of symmetry (see Figures 1 and 3). Following this idea, an experimental setup (see Fig. 5) for simulating wave propagation in these structures was formed by a 36-mm-length square waveguide of width  $a = 6$  mm (cutoff frequency at 25 GHz), loaded by an array of seven BC-SRRs placed at the center of the waveguide (with the geometrical pa-

rameters shown in Figure 2 and with the BC-SRR spacing also set to  $a = 6$  mm). The input and output were two commercial coaxial to rectangular waveguide transitions. The measured  $|S_{12}|$  results shown in Figure 5 present a sharp passband above the resonance frequency of an individual BC-SRR. The bandwidth is also approximately accounted for by the numerical predictions. The agreement between the numerical and experimental results allows to conclude that the proposed structure actually behaves as a left-handed medium.

Additional support for this conclusion has been obtained by measuring the  $|S_{12}|$  for different-length BC-SRR loaded square waveguides having different numbers of BC-SRRs. In all cases, both the bandwidth and the absolute value of the  $|S_{12}|$  were substantially the same. This fact supports the conclusion that this passband is due to the presence of an effective almost-lossless homogeneous medium between the input and the output. It should be also noticed that the passband is located *above* the resonance frequency of an individual BC-SRR. Since causality imposes that negative magnetic permeability for resonant media should always take place *above* the resonance, this fact strengthens the aforementioned interpretation of the experimental results.

### 4. CONCLUSIONS

A novel design for an isotropic 2D left-handed artificial medium (metamaterial) has been proposed. One of the main advantages of the present proposal is that it considerably simplifies previous designs. Simplification arises from the fact that all metallizations are arranged in parallel planes. Thus, the whole structure can be built via the widely used planar technology. Broadside-coupled SRRs are used instead of edge-coupled SRRs in order to ensure the isotropy of the medium. An analytical model for the behavior of this novel metamaterial has been also provided. This study has been complemented with numerical calculations based on the proposed model and experimental validation of the model, which takes advantage of the possibility of simulating the 2D medium by

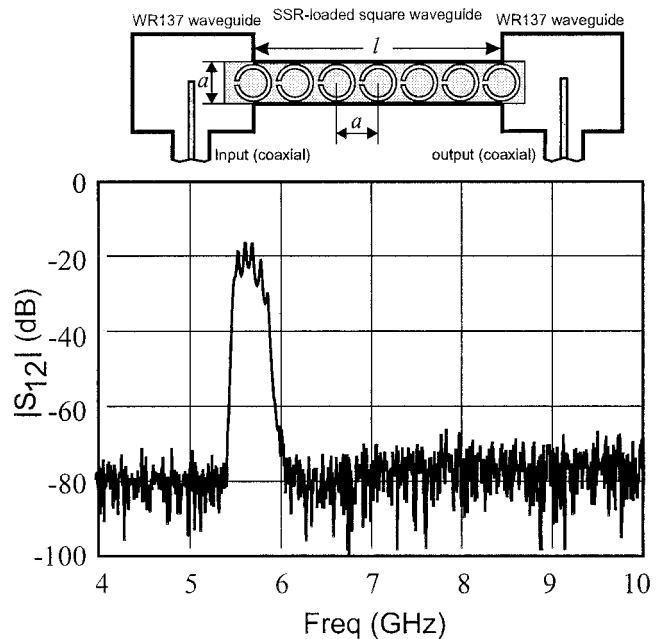


**Figure 5** Experimental setup and experimental data for the  $|S_{12}|$  as a function of frequency. The distance between the BC-SRRs in the waveguide and the internal size of the square waveguide walls are both equal to  $a = 6$  mm

a 1D BC-SRR loaded square waveguide. The proposed 2D metamaterial is expected to be useful for experimentation on negative refractive index and planar lenses made with this new left-handed medium. It should be also noticed that the reported transmission of electromagnetic waves through BC-SRR-loaded metallic waveguide, at frequencies far below cutoff, may also find applications in the design of new microwave devices, such as miniaturized waveguides and filters.

## ACKNOWLEDGMENTS

This work has been supported by the Spanish Ministry of Science and Technology and FEDER funds.

## REFERENCES

1. V.G. Veselago, Electrodynamics of substances with simultaneously negative electrical and magnetic permeabilities, *Sov Phys Usp* 10 (1968), 509–517.
2. D.R. Smith, W.J. Padilla, D.C. Vier, S.C. Nemat-Nasser, and S. Schultz, Composite medium with simultaneously negative permeability and permittivity, *Phys Rev Lett* 84 (2000), 4184–4187.
3. J.B. Pendry, A.J. Holden, D.J. Robbins, and W.J. Stewart, Magnetism from conductors and enhanced nonlinear phenomena, *IEEE Trans Microwave Theory Tech* 47 (1999), 2075–2084.
4. R.A. Shelby, D.R. Smith, and S. Shultz, Experimental verification of a negative index of refraction, *Science* 126 (2001), 77–79.
5. J.B. Pendry, Negative refraction makes a perfect lens, *Phys Rev Lett* 85 (2000), 3966–3969.
6. R.A. Shelby, D.R. Smith, S.C. Nemat-Nasser, and S. Schultz, Microwave transmission through a two-dimensional, isotropic, left-handed metamaterial, *Appl Phys Lett* 78 (2001), 489–491.
7. R. Marqués, F. Medina, and R. Rafi-El-Idrissi, Role of bianisotropy in negative permeability and left-handed metamaterials *Phys Rev B* 65 (2002), 144440.
8. I. Bahl and P. Bhartia, *Microwave solid state circuit design*. Wiley, 1988.

© 2002 Wiley Periodicals, Inc.

# RADIATION PATTERN CONTROL BY SUBREFLECTOR SHAPING IN A DUAL-REFLECTOR ANTENNA

J. R. Bergmann<sup>1</sup> and L. C. Palma Pereira<sup>2</sup>

<sup>1</sup> CETUC — Center for Telecommunications Studies  
Catholic University of Rio de Janeiro  
RJ 22453-900, Brazil

<sup>2</sup> Radiating Systems Department  
Fundação CPqD  
Campinas, SP, Brazil

Received 24 May 2002

**ABSTRACT:** *Dual-shaped reflector antennas have applications in satellite communications systems in which the highest antenna gain and stringent specifications on cross-polarization are required. For antennas fed by a single feed, the radiation pattern control is obtained either by shaping one of the reflectors or by simultaneously shaping both reflector surfaces. In this paper, we explore the design of Gregorian configurations where the main reflector is an offset paraboloid and the subreflector is shaped so as to attain the coverage specifications. By considering the specifications for a high-efficiency ground-station antenna and a contoured beam antenna, two design examples are presented.* © 2002 Wiley Periodicals, Inc. *Microwave Opt Technol Lett* 35: 408–412, 2002; Published online in Wiley InterScience (www.interscience.wiley.com). DOI 10.1002/mop.10621

**Key words:** *satellite antennas; shaped reflector*

## INTRODUCTION

Dual-shaped reflector antennas have many applications in modern satellite communications systems, especially when stringent requirements for cross-polarization are required. For antennas fed by a single feed, several design examples are presented [1–2], where the radiation pattern control is obtained either by the simultaneous shaping of both reflectors or by the shaping of the main reflector with the subreflector as an offset portion of a conventional conical surface (ellipsoid or hyperboloid). Although, among the above alternatives, the dual-shaped reflector offers the best radiation performance, its costs to manufacture are the highest, especially due to the need of developing a separate scheme for production of the main reflector. Attracted by the possible cost reduction, we consider an alternative configuration where an offset paraboloid main reflector is illuminated by a subreflector that is shaped to attain the coverage specifications. To illustrate the performance of this antenna configuration, we present design examples for two satellite applications: a high-efficiency ground-station antenna and a contoured-beam satellite antenna.

## DUAL REFLECTOR SYNTHESIS TECHNIQUE

The synthesis technique employed herein combines a diffractive analysis and an iterative optimization algorithm to yield the unknown coefficients of expansion in a polynomial-Fourier series used to represent the subreflector surface [2]. The optimization scheme adjusts the coefficients used to describe the subreflector surface to comply with coverage specifications defined on a grid of far-field stations. To alleviate subreflector shaping, this synthesis procedure can also optimize the feed position and the offset angle. For an accurate prediction of the antenna radiation pattern, especially when compact designs operating over large frequency bands are required, it is essential that the feed model incorporate the near field effect. In this synthesis procedure, spherical wave expansions obtained from the measured fields represent the feed near-field radiation pattern.

Convergence of the iterative optimization scheme relies on the choice of the initial solution and of the number of expansion coefficients used to represent the shaped subreflector. The use of a large number of coefficients may ensure an optimum solution, but it may be numerically inefficient. The choice of an adequate number of coefficients depends on the reflector and subreflector sizes, the feed radiation pattern parameters, and the desired antenna radiation characteristics. The choice of an adequate initial solution for the iterations is also essential to control subreflector dimensions, feed blockage, aperture clearance, and the subreflector edge illumination level. The starting solution adopted for the synthesis procedure is the classical offset Cassegrain or Gregorian antenna configuration, where the aperture projection diameter  $D$ , focal length  $F$ , and offset distance  $H$  define the parabolic main reflector, as shown in Figure 1. The axis tilt angle, interfocal distance, and eccentricity describe the conical subreflector. However, in addition to the paraboloid parameters that are previously defined, the usual design inputs for the antenna are the projected subreflector height  $V_S$  in the symmetry plane, the feed subreflector edge angle  $\theta_C$ , and the clearance between the top of the subreflector and the bottom of the main reflector  $d_C$ . The feed offset angle  $\theta_O$  can be used to impose the condition for the feed point direction that yields zero-cross-polarization radiation from a geometrical optics standpoint  $\theta_O = \theta_M$ . Based on [3], a design procedure for these classical offset configurations with a pre-defined main reflector is presented in [4]. It relates the above-